Electrochemical and Spectral Properties of Ferrocene (Fc) in Ionic Liquid: 1-Butyl-3-methylimidazolium Triflimide, [BMIM][NTf2]. Concentration Effects

ARTICLE *in* THE JOURNAL OF PHYSICAL CHEMISTRY B · FEBRUARY 2009

Impact Factor: 3.3 · DOI: 10.1021/jp809095q · Source: PubMed

6 AUTHORS, INCLUDING:

M. A. Vorotyntsev
University of Burgundy
138 PUBLICATIONS **2,906** CITATIONS
SEE PROFILE

Laurent Gaillon
Pierre and Marie Curie University - Paris 6
35 PUBLICATIONS **842** CITATIONS
SEE PROFILE

THE JOURNAL OF PHYSICAL CHEMISTRY B

Article

Electrochemical and Spectral Properties of Ferrocene (Fc) in Ionic Liquid: 1-Butyl-3-methylimidazolium Triflimide, [BMIM][NTf]. Concentration Effects

Mikhail A. Vorotyntsev, Veronika A. Zinovyeva, Dmitry V. Konev, Michel Picquet, Laurent Gaillon, and Cecile Rizzi

J. Phys. Chem. B, **2009**, 113 (4), 1085-1099 • DOI: 10.1021/jp809095q • Publication Date (Web): 07 January 2009

Electrochemical and Spectral Properties of Ferrocene (Fc) in Ionic Liquid: 1-Butyl-3-methylimidazolium Triflimide, [BMIM][NTf_2]. Concentration Effects

Mikhail A. Vorotyntsev,* Veronika A. Zinovyeva, Dmitry V. Konev, and Michel Picquet

ICMUB-UMR 5260 CNRS, University of Bourgogne, Bat. Mirande, 9 avenue A. Savary, BP 47 870, 21078 Dijon Cedex, France

Laurent Gaillon and Cecile Rizzi

UPMC Université Paris 06 UMR 7575, Laboratoire d'Electrochimie et de Chimie Analytique, Paris Cedex 05, France, and CNRS-ENSCP UMR 7575 Laboratoire d'Electrochimie et de Chimie Analytique, case 39, 4 place Jussieu, 75252 Paris Cedex 05, France

Received: October 14, 2008

Several earlier studies of the electrochemical oxidation of ferrocene (Fc) in room-temperature ionic liquids revealed an essentially nonlinear dependence of the oxidation current on the Fc concentration in its relatively dilute solutions, with its formally calculated diffusion coefficient strongly increasing with the concentration. Since no plausible mechanism leading to this very unusual finding had been proposed, our study of Fc solutions in 1-butyl-3-methylimidazolium triflimide, [BMIM][NTf_2], was performed to verify whether the above observation originated from an incorrect determination of the dissolved Fc concentration. Our observations have demonstrated that reliable control of the Fc concentration in solution is complicated by factors such as the low amount of Fc used to prepare small-volume solutions or the great difficulty to dissolve completely a solid powder in a solvent with an extremely high viscosity. An unexpected additional complication is related to a sufficiently high volatility of Fc which manifests itself even at room temperature and especially at elevated temperatures or/and in the course of vacuum treatment of its solutions or its solid powder. Parallel measurements of electrochemical responses and UV−visible spectra for several series of Fc solutions of various concentrations (prepared with the use of different procedures) have shown a perfect parallelism between the peak current and the intensity of the absorption band in the range of 360−550 nm, leading us to the conclusion of a linear relationship between the oxidation current and the molecularly dissolved Fc concentration. The relations of these measured characteristics with the estimated Fc concentration in these solutions have demonstrated a much greater dispersion (attributed to the difficulty of a precise measurement of the latter) but without a significant deviation from the linearity in general. This finding has allowed us to estimate the diffusion coefficient of this species: $D = (1.7 \pm 0.2) \times 10^{-7}$ cm^2/s. The extinction coefficients for the maximum of the absorption band (at 440 nm) of Fc have been compared for a series of solvents: [BMIM][NTf_2], acetonitrile, THF, heptane, CH_2Cl_2, ethanol, and toluene. A simple method to estimate reliably the concentration of solute Fc in ionic liquids based on spectroscopic measurements has been proposed, owing to the proximity of Fc absorption properties for a great variety of solvents.

Introduction

Room-temperature ionic liquids (ILs) have drawn enormous attention during the past decade owing to their advantageous properties:[1−3] high thermal stability,[4] very low vapor pressure[5] and therefore low inflammability, and tunable solubility of organic derivatives[6] or gases.[7] Moreover, although some ILs have proven to be reactive,[8] the structural diversity allowed by the simple combination of cations and anions leads to a general trend of chemical stability to numerous chemical agents (water, oxygen, acids and bases, etc.) of these compounds. Ionic liquids have thus been intensively used as solvents for organic chemistry[9,10] and catalysis.[11−16]

For electrochemical experiments, these media also represent an attractive option, owing to their "potential windows" (which are sufficiently large for many applications), chemical inertness with respect to most reactants, the possibility to deoxygenate them or/and to remove water from them rapidly by vacuum pumping with/without heating, and their sufficiently high electric conductivity which allows one to perform electrochemical measurements without an additional supporting electrolyte.[17,18] These advantageous properties allowed one to use ILs as media for advanced electrochemical devices,[19] electrochemically promoted organic reactions,[20−22] electrodeposition of metals and semiconductors,[23] and electrochemistry of conducting polymers.[24−27] See review[18] for other references.

On the other hand, specific properties of these media (first of all an extremely high viscosity resulting in very slow heat and mass transport processes) lead to various "unusual" features,[28] like a very long period of establishing a stationary or steady-state regime.[29] Besides, a relatively high cost to prepare high-purity ILs leads to the tendency to miniaturize electrochemical cells containing mostly a few milliliter or even submilliliter volumes of this solvent.[30−33] This makes the accurate realization of such experiments more technically complicated, compared to aqueous media or conventional organic solvents.

* Corresponding author, mv@u-bourgogne.fr.

10.1021/jp809095q CCC: $40.75
Published on Web 01/07/2009

The small size of these cells dictates frequent use of metal (mostly Ag or Pt) wires as reference electrodes (RE), instead of those based on a well-established redox reaction. The relation between the potentials measured versus such RE and those with respect to a conventional scale is often based on the measurement of the standard potential for a known solute species with a simple redox mechanism and a relatively weak dependence on solvent properties, first of all for ferrocene (Fc) oxidation in the same medium, as was proposed in ref 34 and recommended for use by IUPAC.[35] In this context a detailed knowledge of this process is of great importance and numerous studies in various ILs have been performed, including those with several 1,3-dialkylimidazolium cations[21,22,30,31,35−42] (M = methyl, E = ethyl, B = butyl): [MMIM], [EMIM], [BMIM], [BBIM], [BEIM]; see review[8] for abbreviation rules.

Similar to the Fc oxidation in numerous molecular organic solvents, all reported electrochemical studies in ILs resulted in the observation of a reversible redox transformation, e.g., a curve of the Randles−Sevcik type for cyclic voltammetry (CV), so that the corresponding analytical formulas for the oxidation current were used to calculate the diffusion coefficient of this species. In most publications the measurement was performed for a single Fc concentration. Several recent studies of the concentration dependence of the steady-state current,[36] of the Cottrell coefficient in the chronoamperometry,[37] or of the peak current in cyclic voltammetry[30,37] carried out in [BMIM][NTf_2] (triflimide anion),[36] [BMIM][BF_4],[37] or [BMIM][PF_6][30] resulted in a surprising observation of a *nonlinear* relation between the Fc concentration and the oxidation current.

All of these publications reported that the current in the concentration range of $10^{-3}-10^{-2}$ M was increasing much more rapidly than the concentration. As a consequence, the diffusion coefficient of Fc in each of these ILs calculated on the basis of the conventional formula for the corresponding technique turned out to be a rapidly increasing function of the concentration, contrary to the constancy of this parameter in the same Fc concentration range in molecular organic solvents.

The dependence of the diffusion coefficient on the concentration may originate from numerous reasons:[36] contribution due to electron exchange between solute Fc and Fc^+ (oxidation product) species, migration transport, increase of the solution density, and viscosity changes. However, it was concluded that none of these factors could be responsible for the above *strong nonlinearity* in the current−concentration relation.

Our study represents an attempt to clarify the origin of this paradoxical finding. In view of a compact molecular structure of Fc, the absence of an electric charge, no indications of a specific adsorption at the electrode surface (the shape of the CV curves corresponds perfectly to a diffusion-controlled reversible process, no dependence on the electrode material), and the range of low concentrations (in which the average distance between the neighboring solute Fc species is about 30−100 Å, very far beyond the molecular scale), it looks hardly real to attribute it to an *interaction between solute molecules* (directly or via the medium) which is necessary for any nonlinear effect.

Therefore, a starting hypothesis of this study was that *the real concentrations of Fc* in studied solutions might be different from the expected ones. An evident technical problem is a relatively small amount of the substance. Besides, the process of its dissolution in an IL is much slower than that in conventional organic solvents. Other complications specific for the system under consideration were only discovered in the course of this work.

To answer to the above principal question without any ambiguity related to the concentration determination, we decided to perform parallel measurements of *two* characteristics of Fc solutions, electrochemical signal and UV−visible spectrum, for the same series of solutions of various concentrations. If the above nonlinearity were related to a specific feature of the electrochemical process, the absorption intensity should demonstrate a linear dependence on the concentration. On the contrary, if the problem originated from the uncertainty of the molecularly dissolved Fc concentration *both* characteristics should show similar deviations from the linear dependences on the estimated concentration while being well correlated *between one another*.

This program was realized for Fc solutions in 1-butyl-3-methylimidazolium triflimide, [BMIM][NTf_2]. This IL possesses a relatively low viscosity and correspondingly high conductivity and diffusion coefficients of dissolved species, compared to, e.g., [BMIM][BF_4] and especially [BMIM][PF_6]. Another important property of this IL is its hydrophobic character which allows one to diminish more easily the water content whose presence may affect strongly the transport properties of the medium.[33]

After the completion of our experimental studies, a recent paper[31] has been published in which the electrochemistry of Fc and cobaltocene complexes in several ILs (including [BMIM][NTf_2]) was characterized with the use of double potential step experiments at a microelectrode in a two-electrode configuration. Comparison of our findings with these results is given in section 7 (Discussion).

Results and Discussion

1. Shape of Voltammograms. Scan-Rate Dependence. In view of our preliminary hypothesis that the previously observed nonlinearity in the relation between the oxidation current and the Fc concentration might originate from the difficulty to control reliably the latter, especial attention was paid to the search of the way to prepare Fc+IL solutions which would provide the best estimation of the obtained concentration of the solute Fc. Three different procedures were used, each of them having its merits and shortcomings, resulting in three series of measurements for solutions of a progressively increasing concentration (in each series); see Appendix 3 for a detailed description of these procedures.

Each solution in all series was characterized by means of two techniques: cyclic voltammetry in the range of the Fc/Fc^+ transition and UV−vis−NIR spectroscopy in the interval from 190 to 1100 nm. All CV curves in the figures below correspond to the first cycle after the system's relaxation at a sufficiently negative potential, −(0.3−0.5) V.

In conformity with the published data for Fc in imidazolium ILs with various anions,[22,37,39] all registered CVs corresponded well to a reversible one-electron process controlled by diffusion. The anodic peak current is proportional to the square route of the scan rate, v (Figure 1a). If the current of a CV is divided by $v^{1/2}$ the "reduced voltammograms" for various scan rates become practically coincident within the whole potential interval, as one can see in Figure 1b for the values of v from 3 mV/s and higher. The upper limit is determined by Ohmic losses inside the bulk solution (1.5−2 kΩ for Pt disk electrode, 0.5−0.6 kΩ for glassy carbon (GC) electrode): if the IR compensation mode of the potentiostat is used (curves 4 and 5 in Figure 1b for 10 and 100 mV/s), the corresponding "reduced CV curves" overlap well with that for 5 mV/s. For this relatively high Fc concentration, the peak currents for these higher scan rates are already in the

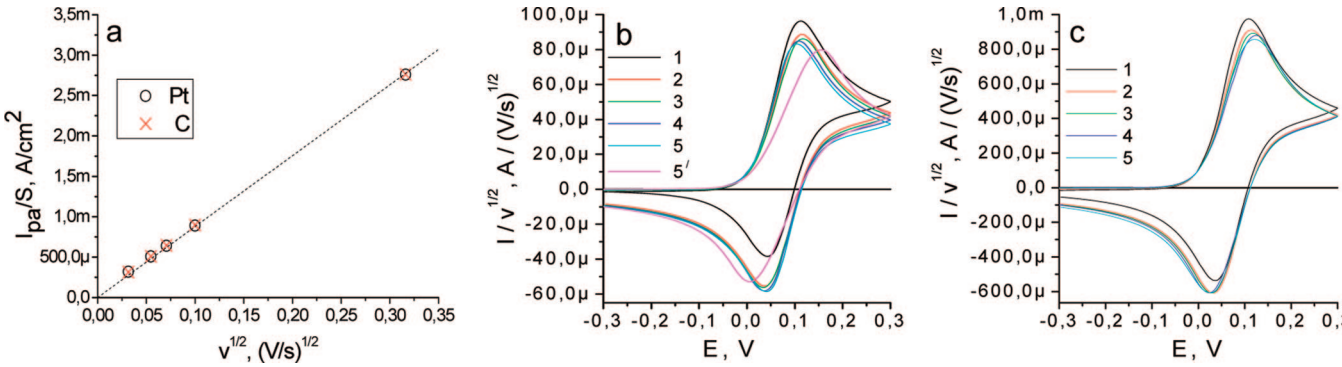

Figure 1. Relation between the oxidation peak current density, I_{pa}/S, and $v^{1/2}$ for Pt and GC electrodes (a). "Reduced CV curves", $I/v^{1/2}$ vs E, for Pt (b) and GC (c) electrodes, scan rate $v = 1$ (curve 1), 3 (curve 2), 5 (curve 3), 10 (curve 4), or 100 mV/s (curves 5 and 5′). IR compensation was used: (b) Pt electrode, $R = 980\ \Omega$ (curve 4) or 1510 Ω (curve 5); (c) GC electrode, $R = 300\ \Omega$ (curves 1−4) or 450 Ω (curve 5).

range of tens of microamperes (despite the small size of the Pt electrode surface area, below 0.01 cm^2) so that the CVs measured without IR compensation (curve 5′ in Figure 1b) demonstrate a marked shift of their anodic and cathodic peaks as well as the diminution of their intensities, due to Ohmic potential drop inside bulk IL.

A specific feature of CVs in ILs is the possibility to use this technique (without effects due to the convective motion of solution) for much lower scan rates, down to about 3 mV/s in Figure 1b, compared to about 20 mV/s for molecular solvents. It reflects directly a much longer relaxation time of the diffusion layer in ILs,[29] due to a much lower value of the diffusion coefficient. For an even slower scan rate, 1 mV/s, Figure 1b shows a higher "reduced current" in the anodic branch and a smaller one (with the absence of the "diffusional tail" after the cathodic peak) in the cathodic scan, in comparison with "reduced CV" for higher scan rates. All these effects are related to a greater thickness of the nonstationary diffusion layer for 1 mV/s whose external area is already influenced by the solution convection which accelerates the Fc transport to the surface during the anodic scan but diminishes the concentration of the product, Fc^+, inside the diffusion layer during the backward scan, especially after the passage of the cathodic peak.

The absence of kinetic (in the electron-transfer step) or adsorption effects in this process is also confirmed by the identical observations for different working electrodes (WE), Pt and glassy carbon, e.g., the coincidence of the linear dependences of the peak current density on the scan rate (Figure 1a) or of the "reduced CV curves" in Figure 1, panels b and c.

In the absence of Ohmic losses, especially for lower Fc concentrations or/and slow scan rates, the anodic and cathodic peak potentials are independent of the scan rate or of the Fc concentration, with the middle potential $E_{1/2} \cong 0.077-0.082$ V vs Ag/0.01 M $AgNO_3$ + AN (Appendix 2). The difference between the peak potentials, 60−65 mV, is not far from the theoretical value for a perfectly reversible electron-transfer process.

The verification of the Nicholson reversibility criterion[43] showed a practical identity of the values of the "forward" and "corrected backward" peak currents: $I_{pc}^*/I_{pa} \cong 1$, thus confirming this conclusion. A more detailed analysis is carried out in Figure 2 in which the experimental CV curve for 10 mV/s is compared with the simulated one. The latter was obtained by fitting the experimental curve with varying the parameter $E°$ (responsible for the values of the peak potentials) and the product $D^{1/2}cS$ (regulating the intensity of the current, see eq 1 in the next section), the electron-transfer rate constant being sufficiently great to make the simulated curve independent of this parameter.

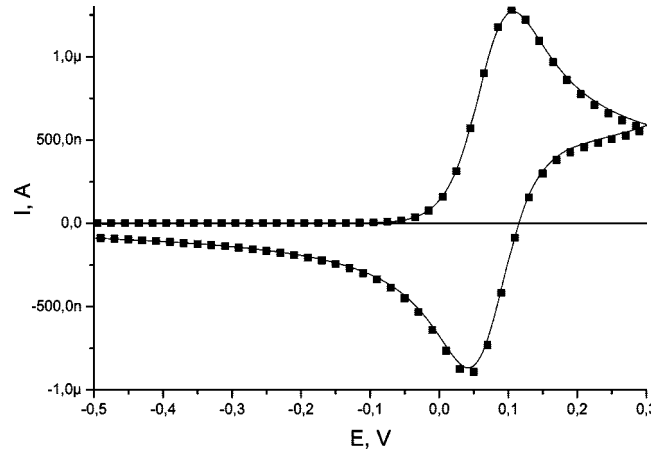

Figure 2. Comparison of the measured (line) and simulated (points) CV curves for 8.9 mM Fc+IL solution (series 2). Pt electrode, 10 mV/s. Simulation parameters determined by fitting: $E° = 0.077$ V, $D^{1/2}cS = 4.8 \times 10^{-8}$ M cm^3/s$^{1/2}$.

The agreement of the curves is almost perfect; one can only notice a very small upward shift of the measured data near the anodic limit of the scan and near the cathodic peak. These (systematically observed) deviations may originate from convection or/and "electrode edge" effects leading to a slight acceleration of the Fc transport to the electrode for the most positive potentials as well as to some loss of the reaction product, Fc^+, to the bulk solution. Thus, similar to the Fc oxidation in usual solvents this process represents an etalon example of a perfectly reversible electron transfer without chemical steps.

2. Concentrational Dependence. Series 1. For the study of the concentration dependence of the electrochemical and spectroscopic responses, series 1 of solutions was prepared on the basis of the 10 mM Fc solution in AN whose portions were added progressively, initially to IL, then to the Fc+IL solution prepared at the previous step. This procedure allowed us to avoid such problems as the tendency of the solid Fc powder to remain at the surface of IL or a slow dissolution rate of solid Fc particles inside IL because of a very slow diffusional transport of dissolved Fc molecules from the surface of the particle. AN was chosen as perfectly miscible with this IL while being sufficiently volatile to remove it later from the mixed solution by vacuum pumping. The amount of Fc transferred into the mixed solution was reliably controlled by the volume of the added Fc+AN solution.

Such additions of the 10 mM Fc+AN solution were made stepwise, to obtain a series of solutions corresponding expectedly

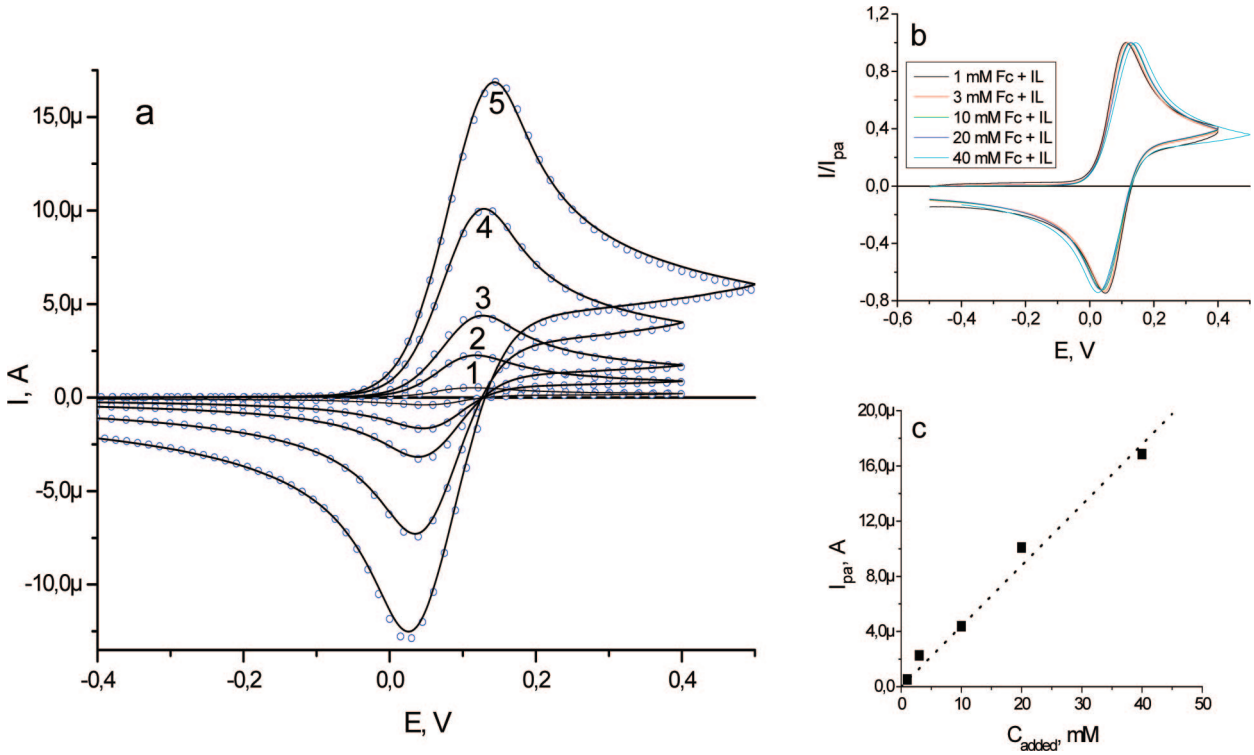

Figure 3. (a) Measured (lines) and simulated (points) CV curves for the Fc+IL solutions of series 1 corresponding to 1 (curve 1), 3 (curve 2), 10 (curve 3), 20 (curve 4), and 40 (curve 5) mM "added concentrations" (calculated with the use of the amounts of added Fc and of the IL), Pt electrode, 100 mV/s. (b) Set of "normalized" experimental curves of Figure 3a (division by the corresponding peak current), I/I_{pa} vs E. (c) Relation between the oxidation peak current, I_{pa} (corrected for the EDL capacitive charging) and the "added concentrations", c_{added}.

to the concentrations of 1, 3, 10, 20, and 40 mM, these estimations being based on the added amounts of Fc and the initial volume of IL (2.5 mL). After each addition the mixed Fc+AN+IL solution was subject to the vacuum pumping for the time sufficient to remove AN (see detailed description in Appendix 3). Thus obtained Fc+IL solution was characterized with the CV and spectroscopic techniques.

A set of CV curves for all solutions of this series (for the same scan rate, 100 mV/s) is given in Figure 3a. The shape of each curve corresponds well to the analysis in section 1. This conclusion was confirmed by the comparison with the simulated CV curves (Figure 3a) calculated for mechanism E_{rev}, i.e., the simple electron-transfer process with a sufficiently high value of the heterogeneous reaction rate constant so that the overall reaction rate is controlled by the diffusion of Fc or of the reaction product, Fc^+.

The whole set of theoretical CV curves in Figure 3a was obtained for the identical values of parameters of the process: $E_{1/2} \equiv E^\circ + (RT/2F)\log(D/D_{Fc+}) = 0.082$ V (determining the middle potential of each CV) and the resistance of the bulk solution, $R = 1600\ \Omega$, while the value of the product, $D^{1/2}cS$ (see eq 1 below) was found by fitting separately for each experimental CV curve: 0.61×10^{-8} (curve 1), 2.7×10^{-8} (curve 2), 5.3×10^{-8} (curve 3), 12.3×10^{-8} (curve 4), and 21.2×10^{-8} M cm^3/s$^{1/2}$ (curve 5). The latter values result in the ratio of Fc concentrations for these solutions on the basis of these electrochemical data: 1:4.4:8.7:20.2:34.6.

Figure 3b demonstrates a very close proximity of the shapes of various experimental curves (their currents were divided by the corresponding anodic peak current), the only difference being a progressive displacement of both waves from $E_{1/2}$ with increase of Fc concentration. This effect perfectly reproduced in the simulated curves of Figure 3a is due to the Ohmic potential drop in the bulk solution.

Figure 3c presents the dependence of the oxidation peak current, I_{pa}, on the "added concentrations" of Fc. Contrary to the previous publications where a strong *upward* deviation from the linear dependence was reported, Figure 3c does not show a pronounced curvature but rather a dispersion of points with respect to a straight line. Its slope might be used to calculate the diffusion coefficient of Fc in this IL, D, with the use of the Randles−Sevcik formula for the peak current for the E_{rev} mechanism

$$I_{pa} = (2.69 \times 10^5)D^{1/2}n^{3/2}Scv^{1/2} \qquad (1)$$

Here, peak current, I_{pa}, is measured in μA, D in cm^2/s, surface area, S, in cm^2, concentration, c, in mM, and scan rate, v, in V/s and the number of transferred electrons, n, equals 1. However, the precision of this value would not be high because of the dispersion of the points in Figure 3c. Besides, there is an open question on the reason(s) for this dispersion, due to either an insufficient precision in the values of I or c or a nonlinearity of the relation between these characteristics.

To clarify this point, the UV−visible spectra of the same solutions were registered (the procedure is described in Appendix 2); see Figure 4a. In all spectra one can notice a band in the visible range between 360 and 530 nm, with the maximum absorption near 440 nm, as well as another band (around 325 nm) as a shoulder of a rapidly increasing branch below 300 nm, similar to the Fc spectrum in usual media;[44] see also section 5. If these spectral curves are "normalized" by means of their division by their absorbance at 440 nm, $A(\lambda)/A_{440}$, one can observe a perfect coincidence of all "normalized plots" (Figure 4b). It represents extra evidence in favor of the absence of noticeable interactions between solute Fc molecules so that the Beer−Lambert law for the absorbance, A

$$A = \varepsilon L c \quad (2)$$

containing the extinction coefficient of Fc in this IL, ε, the optical path, L (0.2 cm), and the concentration of solute Fc, c, should be valid. Figure 4c shows the dependence of the absorbance at the band maximum, 440 nm, for this series of solutions on the "added concentration" of Fc, c_{added}. Analogously to the similar relation between the peak currents and the same series of concentrations in Figure 3c, the points in Figure 4c do not demonstrate a clear deviation from a straight line while a significant dispersion is obvious.

For a definitive answer on the origin of this dispersion, the relation between the peak current and the maximum absorbance was analyzed in Figure 4d. All points fit nicely to a straight line passing through the origin, without a significant dispersion. This finding allowed us to conclude that *both characteristics are proportional to the concentration of the solute Fc* (and consequently proportional to one another) and that the deviation of experimental points in plots 3c and 4c from the straight lines is due to an insufficiently precise determination of this solute Fc concentration in these solutions.

In view of the insufficient precision of the values of the slopes in Figures 3c and 4c, the determination of the principal parameters, D and ε, will be postponed until section 7. Without this information one can only find the *ratios of concentrations* for this series of solutions, assuming the validity of eq 1 or 2 and using the experimental data for I_{pa} or A_{440}: 1:4.3:8.3:19.2:32 and 1:4.2:8.6:18.2:31.9, respectively. These values are close to those found above from the fitting of the whole CV curves in Figure 3a, 1: 4.4:8.7:20.2:34.6. The proximity of the corresponding values on the basis of electrochemical and spectroscopic data is a consequence of a low dispersion for the linear plot in Figure 4d. In other words, it means that if the true concentrations of molecularly dissolved Fc in IL are calculated for each solution from its absorbance data (after having determined the extinction coefficient, ε) they will be practically proportional to the measured values for the corresponding peak currents.

3. Thermal and Vacuum Effects on a Fc+IL Solution. Looking for the reason(s) of the deviation of the molecularly dissolved Fc concentration of a solution (determined electrochemically or spectroscopically) from that calculated on the basis of the amount of Fc added into IL in the form of the Fc+AN solution, we can exclude such factors as significant errors in the amount of added Fc or its slow dissolution in IL (which might take place for the direct dissolution of the solid Fc powder in IL). Insufficient solubility of Fc in IL (after AN evaporation) might affect the data but only for highest concentrations while the deviation was observed even for low concentrations. As for incomplete removal of AN, it could affect significantly the electrochemical signal but not the spectral one while a perfect linearity of these parameters was observed within the whole series.

To get further insight, we checked the chemical stability of Fc in this IL by analyzing the effect of the treatment of a 5 mM Fc solution in IL (obtained by direct dissolution of Fc powder) at elevated temperatures or/and by vacuum. When the solution was kept at 50 or 80 °C (including its exposure to vacuum) inside a spectroscopic cuvette *without mechanical stirring*, the spectrum of the solution, and thus the Fc concentration, remained unchanged; i.e., the Fc solution did not degrade within this temperature interval. On the contrary, when the same procedure: heating up to 80° or even 50 °C or vacuum pumping (upon elevated or even room temperature) was performed with

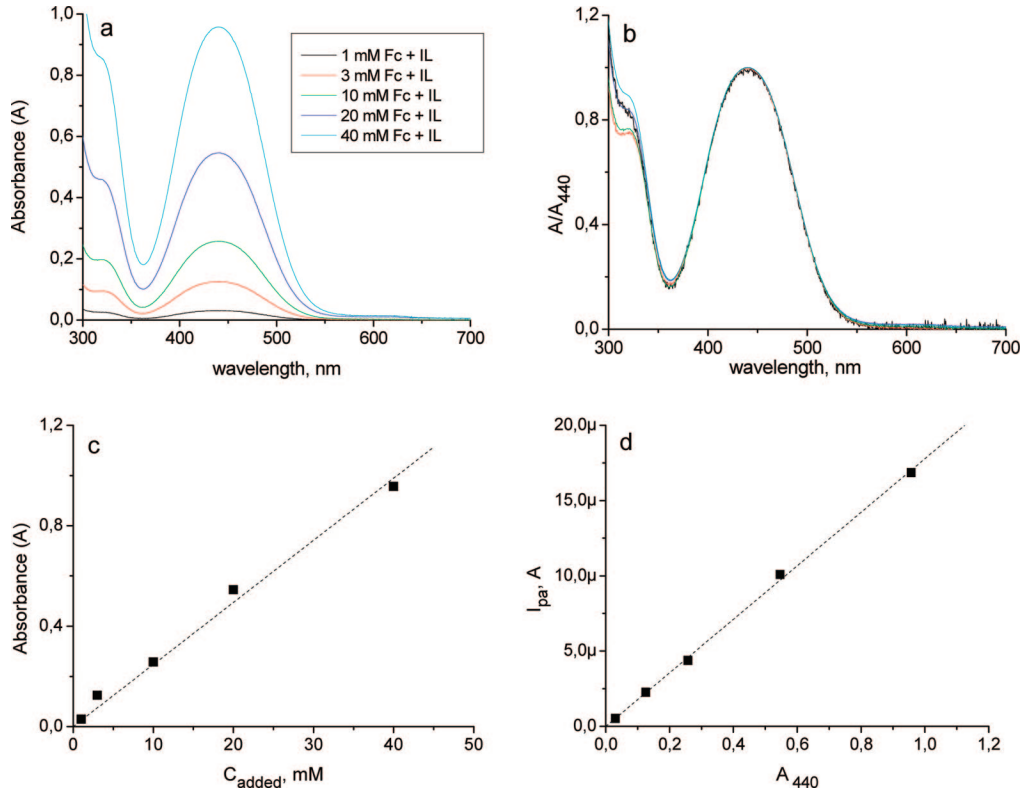

Figure 4. (a) UV−visible spectra for the Fc+IL solutions of series 1 corresponding to 1 (curve 1), 3 (curve 2), 10 (curve 3), 20 (curve 4), and 40 (curve 5) mM "added concentrations". (b) Set of "normalized spectra" (division of curves in Figure 4a by the corresponding maximum absorption), A/A_{440} vs wavelength. (c) Relation between the maximum absorption, A_{440} and the "added concentrations", c_{added} for series 1. (d) Relation between I_{pa} and A_{440} for series 1.

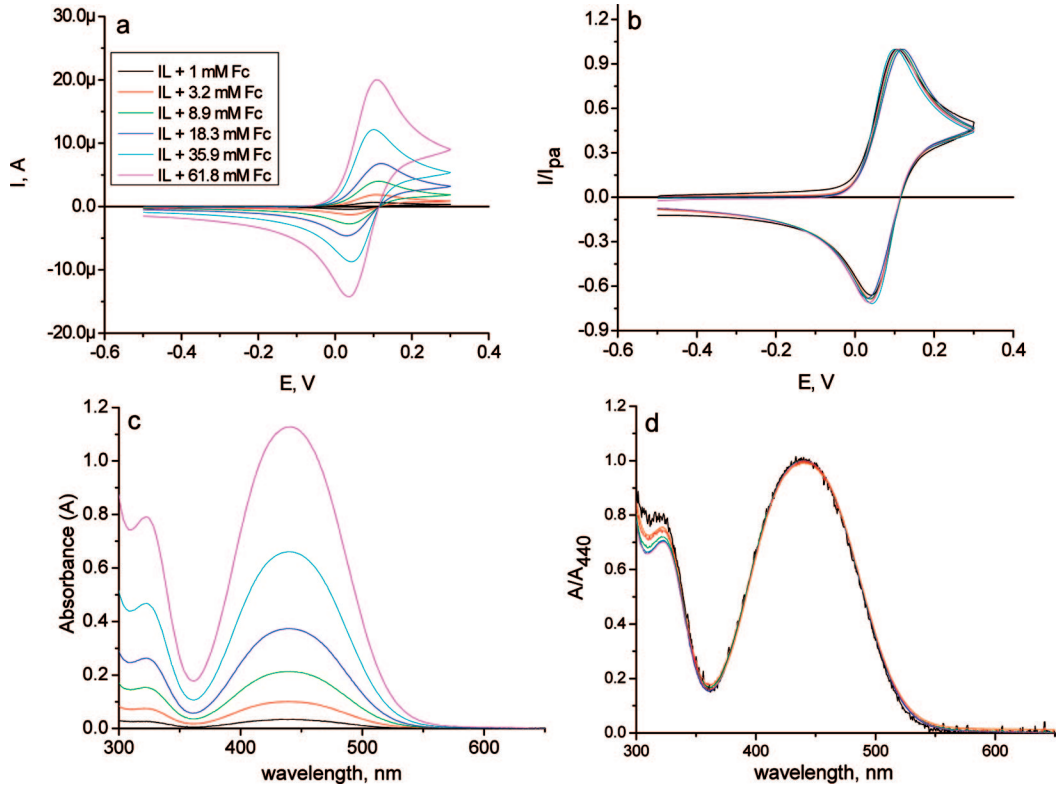

Figure 5. CV curves (a, b) and UV spectra (c, d) for series 2 of Fc+IL solutions. "IR compensation" mode was used for three highest concentrations (1170 or 1510 Ω). In spectral curves the "colloidal branch" has been subtracted (Appendix 2, Figure 13b). In panels b and d, the CV or absorption curves were "normalized" (divided by the oxidation peak current, I_{pa}, or by the (maximal) absorbance at 440 nm, A_{440}, respectively, for the same solution). For the sake of comparison, Figure 5d presents also a typical normalized plot for series 1 (orange curve).

the same solution, placed into the cell *with solution stirring*, the concentration of Fc diminished progressively. Besides, yellow traces of Fc were noticeable on the walls of the vacuum line while the solvent (AN) condensed in the trap (cooled by liquid nitrogen) at the exit of the line was yellow colored. The estimation of the amount of solid Fc inside the Fc+AN solution in the trap by measuring the weight of the solid Fc left after the AN evaporation showed its (crude) correspondence to the amount of Fc lost by the Fc+IL solution in the cell (estimated on the basis of the spectral data) during this treatment.

These observations led us to the conclusion that one of the principal reasons of the difference between the "added" and dissolved Fc concentrations may originate from its *relatively high volatility*, already noted in ref 44 (see also a recent study in ref 45) and which is comparable with, or even higher (depending on the specific treatment) than, that of such viscous solvents as carbonates. It is noteworthy that a rapid diminution of the mass of the *solid Fc* can be easily observed during its heating or vacuum treatment.

The absence of this evaporation inside a Fc+IL solution *without stirring* is obviously related to a very high viscosity of IL and low diffusivity of Fc in IL so that its transport to the free surface of IL limits the rate of this process. The latter can be accelerated not only by mechanical stirring but also by ultrasonic treatment (accompanied by an elevated temperature), bubble formation during the AN removal from IL, or passage of a gas (Ar, N_2) through the Fc+IL solution.

4. Concentrational Dependence. Series 2. This series of concentrations was obtained by direct dissolution of progressively added portions of solid Fc powder inside IL, corresponding to "added concentrations" (after correction for the losses of IL, see Appendix 3 for a detailed description): 1.0, 3.2, 8.9, 18.3, 35.9, and 61.8 mM. Figure 5 presents the electrochemical and spectroscopic data for all these solutions.

The set of CV curves in Figure 5a looks quite analogous to that for series 1 (Figure 3a), the only difference being a smaller shift of both anodic and cathodic peaks to higher potentials for the three highest concentrations, due to the use of the potentiostat mode "IR compensation. Similarly, the "normalization" of these curves (Figure 5b) shows a perfect identity of the shapes of all these CV curves, except for a minor shift of some curves as a whole due to Ohmic potential drop in the bulk solution.

The general shape of the spectral curves for this series of solutions was also very similar to that for series 1 (Figure 4), except for a "colloidal branch" obviously visible within the whole range of wavelengths above 550 nm which was relatively much weaker for series 1. The intensity of this long-wavelength absorption related to insoluble solid microparticles was increasing progressively within the series, roughly proportional to the intensity of the principal band, A_{440}. The recorded spectral curves were corrected by subtraction of this "colloidal branch" from each curve (Appendix 2, Figure 13b), the resulting curves for solute Fc in IL being shown in Figure 5c. The "normalization" of the curves in Figure 5c leads to their perfect overlap within a very broad range of wavelengths including the whole band in the visible range as well as the absorption minimum (at 362 nm) and the beginning of the rapidly raising branch for shorter wavelengths up to 330 nm (Figure 5d).

All these electrochemical and spectroscopic data confirm once again a purely molecular form of the dissolved Fc while attributing the variation of the intensities of these two signals within the series to the progressive increase of the concentration of the solute Fc. As a further verification of this conclusion, the values of the oxidation peak current, I_{pa}, in Figure 5a were

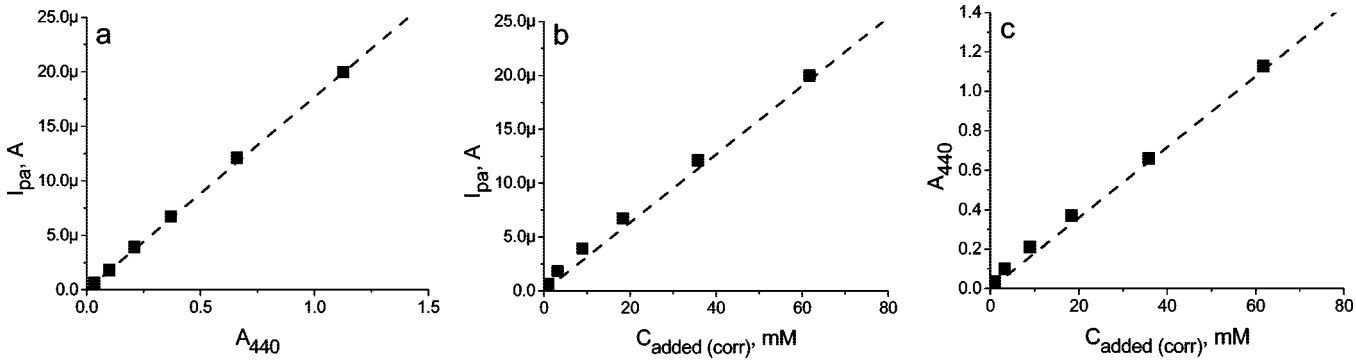

Figure 6. Correlation of the electrochemical, spectral and Fc concentration data for series 2 (Figure 5a,c): (a) I_{pa} vs A_{440}; (b) I_{pa} vs $c_{added(corr)}$; (c) A_{440} vs $c_{added(corr)}$, the values of the "added concentration", $c_{added(corr)}$, being determined from the weight and volume measurements in the course of the solution preparation procedure, with taking into account the corrections for losses of IL (Appendix 3).

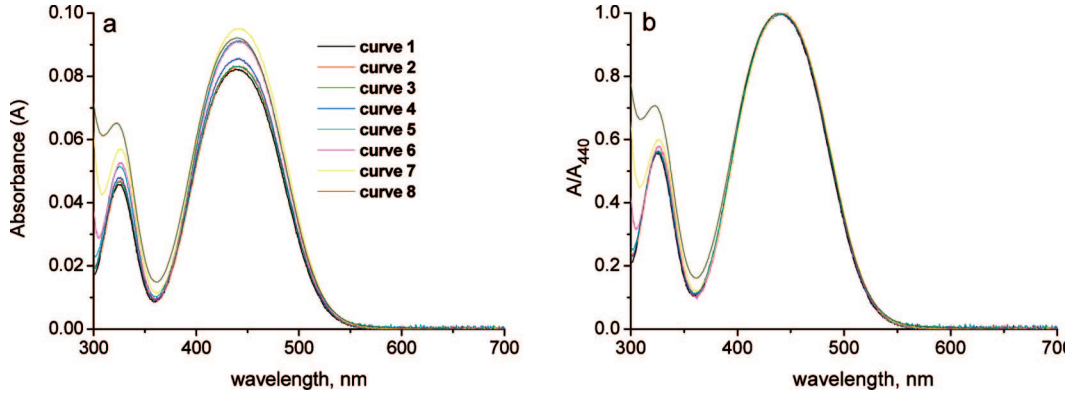

Figure 7. (a) Spectra of 5 mM Fc in various solvents (measured vs the cuvette with the corresponding solvent): heptane (1), THF (2), ethanol (3), ethanol + 1 M $LiClO_4$ (4), AN (5), toluene (6), CH_2Cl_2 (7), [BMIM][NTf_2] (8). (b) Normalized spectra, A/A_{440}, where A_{440} is absorbance at 440 nm in the corresponding Fc solution.

plotted (Figure 6a) versus the corresponding absorbance values at 440 nm (near the maximum of the band) in Figure 5c. Similar to the same plots for series 1 (Figure 4d), a perfectly linear plot passing through the origin is observed. We may again conclude that both measured quantities are determined by the amount of molecularly dissolved Fc and proportional to its concentration in the corresponding solution.

Also analogous to the findings for series 1 (Figures 3c and 4c), the linear relation between the peak current, I_{pa}, or the absorbance maximum, A_{440}, and the Fc concentration determined from the amount of dissolved Fc (even with correction for losses of IL in the course of manipulations, Appendix 3), $c_{added(corr)}$, is much worse (Figure 6, panels b and c), pointing again to the great difficulty to determine the Fc concentration in solution on the basis of the solution-preparation procedure.

5. Spectral Properties of Fc: Solvent Effects. The "colloidal tail" (absorption in the range above 650 nm) was practically absent in the spectra of series 1 of Fc+IL solutions which were obtained by adding portions of the Fc+AN solution to IL. In this context, the observation of a significant "colloidal tail" in the spectra for series 2 obtained by direct dissolution of solid Fc in IL, with the amplitude of this tail increasing in parallel to the amount of added Fc, led us initially to the assumption that this colloid is formed by solid Fc microparticles whose dissolution rate is too slow, due to a very high viscosity of IL. However, the direct dissolution of the solid Fc from the same "new batch" (Appendix 3) in AN, CH_2Cl_2, and other organic solvents revealed the same colloidal tail of a similar intensity in the spectra of these Fc solutions.

The presence of a significant insoluble fraction inside the solid Fc powder resulted obviously to an uncertainty in the amount of Fc dissolved inside IL. Therefore, we tried to remove this fraction by filtration of saturated Fc solution in CH_2Cl_2 through adsorbent (Celite) giving the minimum contamination of the passed solution, according to its UV−vis spectrum (Figure 14, Appendix 3). Then, the solvent was evaporated and the solid Fc was used for preparation of solutions in various solvents, including those in IL (series 3 below).

The filtration resulted indeed in a drastic diminution of the absorbance in the range above 650 nm in all solvents. Besides, the residual absorbance in this range is practically wavelength independent so that this colloidal contribution can be immediately removed by subtraction of this constant value from the spectrum at all wavelengths. The resulting spectra for a set of solvents are given in Figure 7a.

Their normalization (division of each spectrum by its value at 440 nm) gives the same plot for wavelengths above 325 nm in all studied solvents (Figure 7b) which testifies in favor of the same absorbing species, molecular Fc, in all these media, owing to the electronic transition between the states deeply inside this complex, without spreading into the ligands. The only (and rather slight) effect of the solvent nature is in the intensity of the spectrum.

The corresponding extinction coefficients for each solvent are given in Table 1. All these values (including IL) are in a narrow range, 82−95, being in conformity with the literature, e.g., ref 44.

6. Concentrational Dependence. Series 3. The filtrated Fc powder obtained after evaporation of dichloromethane is soluble in all media much faster than the initial solid Fc. Therefore, it was used for preparation of series 3 of Fc+IL solutions by its direct dissolution in this solvent (Appendix 3). Then electro-

TABLE 1: Extinction Coefficients of Solute Fc at 440 nm (near the Maximum of Its Absorption Band in All Solvents)

	C_7H_{16}	THF	C_2H_5OH	C_2H_5OH + 1 M $LiClO_4$	AN	$C_6H_5CH_3$	CH_2Cl_2	[BMIM] [NTf_2]
ε_{440}	82	83	83	85	91	91	95[a]	94 ± 5[b]

[a] This value for CH_2Cl_2 represents its upper estimate, because of rapid evaporation of this solvent. [b] Found in section 7.

chemical and spectroscopic measurements were performed for each solution.

The set of CV curves were quite similar to those for series 1 and 2. On the contrary, the shape of their absorption spectra turned out to be different: in addition to the conventional bands for solute Fc and a weak "colloidal tail" of a constant intensity above 650 nm, a new absorption band appeared in the range 500−650 nm, with maximum at 620 nm (Figure 8a).

The same normalization procedure (Figure 8b) demonstrates the presence of additional species absorbing in the range both 500−650 nm and below 400 nm. We did not find a reliable way to remove these new species (without replacing them in solution with other contaminations) by vacuum or thermal treatment or by the solution filtration through adsorbents (carbon, silica, Celite, cotton, or their combinations). Therefore, the intensity of the absorption band related to Fc was determined by subtraction of the Fc spectrum in IL (known from series 1 and 2) multiplied by an adjusting factor from experimental plots in Figure 8a (Figure 13a in Appendix 2). This treatment showed that in the central area of the Fc band (near 440 nm) there is practically no absorption by the new species so that the value at 440 nm, A_{440}, may be considered as previously as the optical parameter proportional to the concentration of the solute Fc.

As a tentative hypothesis on the origin of this extra absorption in Figure 8a, one may point out a similarity between this additional absorption (compared to pure Fc) and the spectrum of ferrocenium cation, Fc^+, which possesses an absorption band in the visible range (with maximum at 617−619 nm)[44,46−48] and a growing absorption branch in the near-UV range, with no significant absorption between 400 and 450 nm.[46,47,49] One may assume that the passage of the CH_2Cl_2 solution through the adsorbent resulted in extraction of a substance which does not absorb practically in the range above 300 nm and does not interact with Fc dissolved in this solvent, while it oxidizes Fc partially after their dissolution in IL.

This attribution is also confirmed by the measurements of the open-circuit potential of these Fc+IL solutions. These data allowed us to estimate (with the use of the Nernst equation) the ratio of the concentrations of solute Fc and Fc^+ species, the oxidized form being in the range of 1−2% of the total amount. Qualitatively similar estimates of this ratio for the same solutions were also obtained on the basis of the measured absorbances at 440 and 619 nm (Figure 8a) divided by the corresponding extinction coefficients in organic/aqueous solvents (about 90 and 360 M^{-1} cm^{-1}, respectively[44]).

In this context the filtration procedure is probably not optimal for the removal of insoluble component from commercial solid Fc. Our preliminary tests with a portion of Fc subject to sublimation showed that both above problems (colloidal tail and absorption band with a maximum at 619 nm in the spectrum) were still present.

The use of the I_{pa} and A_{440} values for this series 3 of solutions resulted in the same observations as for series 1 and 2: a perfect proportionality between I_{pa} and A_{440} (Figure 9a) and approximately linear relations (but with a much greater dispersion) for I_{pa} vs $c_{added(corr)}$ (Figure 9b) and A_{440} vs $c_{added(corr)}$ (Figure 9c) where the values of concentrations, $c_{added(corr)}$, are found from the solution preparation procedure.

7. Discussion. The superposition of the data for all three series inside a single plot allowed us to extract more reliably the parameters of this system. In particular, all points for the relation between I_{pa} and A_{440} are very close to a single straight line. A much stricter verification of the proportionality is realized in the plot of I_{pa}/A_{440} vs A_{440} (Figure 10a): all experimental points are very close to the same *constant* with a low dispersion: 18.1 ± 0.3 μA.

With the use of eqs 1 and 2, this constant allowed us to find the ratio of the principal electrochemical and absorption parameters of Fc in IL with great precision

$$D/(\varepsilon_{440})^2 = (1.98 \pm 0.07) \times 10^{-11} \quad (3)$$

where D is measured in cm^2/s and ε_{440} in M^{-1} cm^{-1}. A much greater dispersion around straight lines is observed for I_{pa} vs c_{added} (Figure 10b) and A_{440} vs c_{added} (Figure 10c) dependencies. Their slopes according to eqs 1 and 2 estimate these parameters separately

$$D = (1.7 \pm 0.2) \times 10^{-7}\ cm^2/s \quad (4)$$

$$\varepsilon_{440} = 94 \pm 5\ M^{-1}\ cm^{-1}$$

This treatment identified the values of the solute Fc concentration in the corresponding solution, c, in eqs 1 and 2 with those found from the solution preparation procedure, $c_{added(corr).}$ Since the latter values are subject to a much greater dispersion due to numerous origins, the estimation of both parameters in eq 4 should be less precise than that of their ratio in eq 3.

Our conclusion on the applicability of the conventional electrochemical relation, eq 1, for the diffusion of Fc in this IL, its diffusion coefficient being independent of the concentration, is in perfect conformity with the results of recent publication,[31] in which the study was performed at a microelectrode by means of double potential steps. It means that the earlier observations[30,36,37] of a concentration dependence of the Fc diffusion coefficient were due to a difference between the concentration values based on the solution preparation procedure and the real ones in solution, due to numerous technical problems discussed above.

In this context we strongly recommend to determine the real concentrations of solute Fc a posteriori (after the solution preparation). As demonstrated in ref 31, potential step chronoamperometry at a *microelectrode* may serve this purpose, providing simultaneously both the solute concentration and the diffusion coefficient. An alternative approach proposed in our study is based on the measurement of the spectrum in the range of the Fc absorption (near 440 nm) whose intensity is proportional to the solute concentration so that it is sufficient to determine the proportionality coefficient between A_{440} and c. Its advantageous feature is a weak dependence of various contaminations in the IL (traces of water, of organic solvent etc) which manifest themselves in the electrochemical response of Fc at much lower contents, via their strong effect on the IL viscosity. The extinction coefficient of Fc in IL does not vary strongly with temperature (within a few degrees) either, contrary to a drastic temperature dependence of the diffusion coefficient (about 5% per 1 °C).

Moreover, it turned out that the Fc spectra (for an identical concentration) are very similar for various media, including

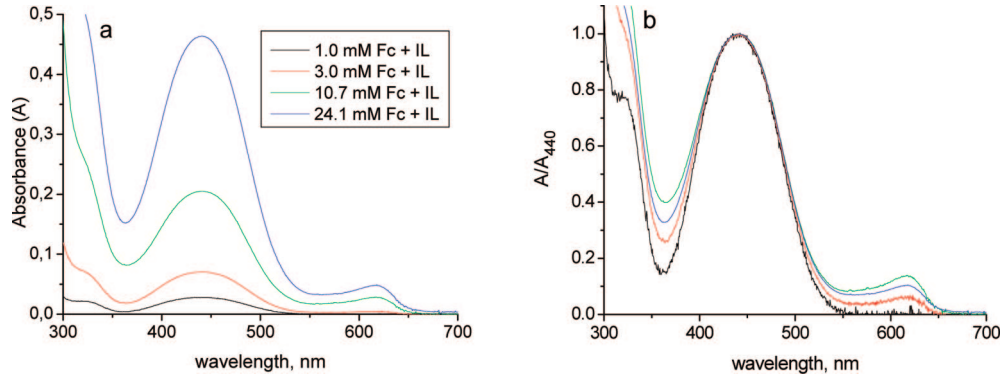

Figure 8. (a) Absorption spectra for Fc+IL solutions (series 3). (b) Normalized spectra, A/A_{440}.

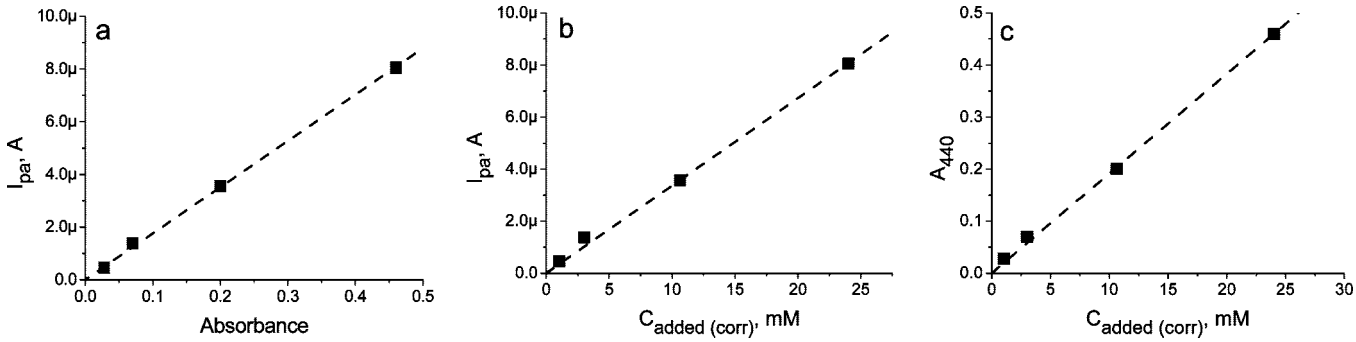

Figure 9. Correlation of electrochemical, spectral and Fc concentration data for series 3: (a) I_{pa} vs A_{440}; (b) I_{pa} vs $c_{added(corr)}$; (c) A_{440} vs $c_{added(corr)}$.

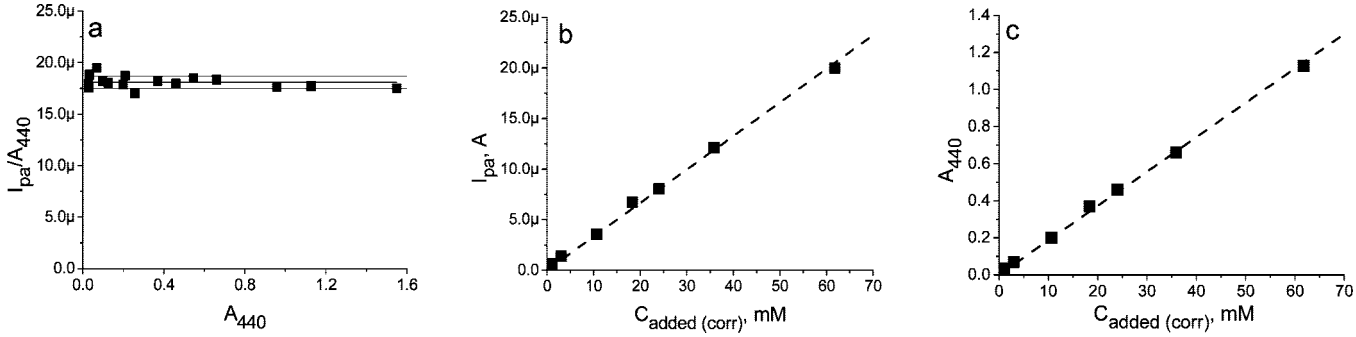

Figure 10. Correlation of electrochemical, spectral, and Fc concentration data for series 2 and 3 of Fc+IL solutions (series 1 was performed without control of the IL losses): (a) I_{pa}/A_{440} vs A_{440}; (b) I_{pa} vs $c_{added(corr)}$; (c) A_{440} vs $c_{added(corr)}$, the values of the added concentration, $c_{added(corr)}$, being determined from the weight and volume measurements in the course of the solution preparation procedure, with taking into account the corrections for losses of IL (Appendix 3).

numerous organic solvents and ILs: not only the band shape in the visible range is the same but even the absorbance at the band maximum (440 nm) is close for all these media so that the values of the extinction coefficient, ε_{440}, are known beforehand with the precision of about 10−15%, even before their measurement for a particular system. Owing to this property, the measurement of two quantities, I_{pa} and A_{440}, for a single Fc solution allows one to calculate the ratio in eq 3, $D/(\varepsilon_{440})^2$, to get from it an approximate but reliable estimation of the diffusion coefficient.

The values for D of Fc in [BMIM][NTf_2] found in ref 31 at 26 °C turned out to be within a narrow interval, (3.6−4.0) × 10^{-7} cm^2/s, for the whole range of the Fc concentrations, 2.8 − 77.4 mM. Our measurements were performed for a lower temperature, 19−21 °C, i.e., at a higher viscosity of the IL (each two-degree shift results in a 10% change of the IL viscosity). Extrapolation of the above finding for D at 26 °C to our temperature range with the use of the activation energy for this quantity, 30 kJ/mol,[31] gives $D = (2.6-3.0) \times 10^{-7}$ cm^2/s, i.e., a higher value than our result. The insertion of this enhanced value into eq 3 results in the estimation, $\varepsilon_{440} = 115-124$, which is markedly above the values for the other media; see Table 1.

Several estimates for the diffusion coefficient of Fc are available for a related IL, [EMIM][NTf_2]: 0.63 × 10^{-7} (T = 20 °C),[22] 3.35 × 10^{-7} (T = 23 °C),[38] and 5.34 × 10^{-7} cm^2/s (T = 26 °C).[31] According to the Stokes−Einstein relation, the values of the product of the diffusion coefficient of a species and the viscosity should be close to each other for similar media. The above results for D and for the viscosity at the corresponding temperature, η = 36.3 cP (20 °C),[50] 32.7 cP[50] or 37 cP[38] (23 °C), and 29.5 cP (26 °C)[50] give for the product, $D\eta$ = 0.23 × 10^{-5}, 1.10 × 10^{-5} or 1.24 × 10^{-5}, and 1.57 × 10^{-5} cP cm^2/s, respectively. Similar calculation for Fc in [BMIM][NTf_2] with the use of our finding for D in eq 4 and the viscosity data for 20 °C, η = 63 cP,[51] results in the value of the product, $D\eta$ = (1.07 ± 0.13) × 10^{-5} cP cm^2/s, which is in a good agreement with the second among the above three values of this product for [EMIM][NTf_2].

SCHEME 1: Structure of [BMIM][NTf_2]

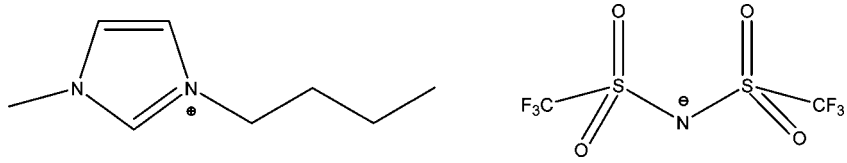

Conclusions

This study has proven that the previously observed anomalies in the dependence of the peak current of the Fc oxidation versus its concentration had originated from a difficulty to determine the concentration of solute Fc on the basis of the solution preparation procedure. This problem is related not only to the small volume of the solution but also to a sufficiently high volatility of Fc, the presence of insoluble microparticles inside the commercial product, the absorption of the solid microparticles by the surface of this highly viscous liquid, etc.

Therefore, we recommend to combine the measurement of electrochemical (or other experimental) parameters of the Fc solution in an ionic liquid with the registration of its spectrum. Then the knowledge of the absorbance at 440 nm and of the extinction coefficient of Fc in this medium, eq 4, allows one to determine reliably the real concentration of the solute Fc.

A great advantage of this approach (compared, e.g., with the concentration determination by electrochemical methods) is owing to rather close values for the extinction coefficient of Fc at 440 nm, 90 ± 8 M^{-1} cm^{-1}, for media whose other properties are extremely different. It implies that various contaminations (e.g., water or organic impurities) or temperatures which influence considerably various transport parameters of an ionic liquid (via its viscosity) do not represent an obstacle for the reliable determination of the Fc concentration.

The measurement of the absorbance for the whole series of solutions (together with registration of other characteristics of the system dependent on the Fc concentration) will allow one to enhance additionally the precision of the study, by the analysis of the linear correlation between these parameters, as demonstrated for the electrochemical and spectroscopic signals.

Acknowledgment. We are thankful to M. Graczyk for helpful advices on electrochemical experiments in ILs as well as to D. Poinsot and E. Pousson for their technical assistance.

Appendix 1. Chemicals

Fc (98%, Aldrich), 1-bromobutane (>99%, ACROS Organics), 1-chlorobutane (>99%, ACROS Organics), and $LiNTf_2$ (>99%, Fluka) were used without additional purification. 1-Methylimidazole (ACROS Organics) was dried over potassium carbonate and distillated prior to use. All organic solvents, acetonitrile (AN, 99.9%, Carlo Erba HPLC grade), ethyl alcohol absolute (99.8%, Carlo Erba ACS—for analysis), tetrahydrofuran (THF, 99+%, pure, stabilized with BHT, ACROS Organics), dichloromethane (stabilized with ca. 100 ppm amylene, ACROS Organics ACS—for analysis), toluene (ACROS Organics ACS—for analysis), *n*-heptane (Carlo Erba RPE—for analysis), were dried and distilled before use, except for ethanol.

Synthesis of [BMIM][NTf_2]. The ionic liquid [BMIM][NTf_2] (Scheme 1) was prepared by reaction of 1-methylimidazole and 1-bromobutane or 1-chlorobutane followed by metathesis with $LiNTf_2$ in water.[52] The resulting product was extracted with dichloromethane and washed several times with water until the $AgNO_3$ test, which allows one to trace even very low contents of halide-based impurities, became negative. Then dichloromethane was evaporated. The residue was lyophilized. The final product was characterized by ^1H (200 MHz, $CDCl_3$) δ (ppm): 1,0 (t, $^3J = 7.3$ Hz, $C\underline{H}_3CH_2$); 1.4 (m, $CH_3C\underline{H}_2CH_2$); 1.9 (m, $C\underline{H}_2CH_2N$); 4.0 (s, $C\underline{H}_3N$); 4.2 (t, $^3J = 7.4$ Hz, $C\underline{H}_2N$); 7.3 (m, H_{Im}); 8.8 (s, H_2), and by mass spectrometry using electrospray (ESI) positive mode $m/z = 138.9$ $[M - NTf_2]^+$, 558.0 $[2M - NTf_2]^+$, and negative mode $m/z = 279.8$ $[M - BMIM]^-$ where M is [BMIM][NTf_2].

Prior to use for Fc solution preparations (Appendix 3) the IL was dried with Schlenk line at 80 °C under vacuum for from 10 h to 2 days. Then IL was kept under argon pressure.

Appendix 2. Electrochemical and Spectroscopic Experiments

For electrochemical experiments, a homemade analogue of the conventional one-compartment glassy cell was constructed which allowed us to decrease the solution volume down to 1.5−2 mL, while retaining the possibility to perform measurements under a deoxygenated atmosphere (vacuum pumping, with the subsequent filling by dry and oxygen-free Ar, then the cell was kept under a slight overpressure of Ar) with the use of three electrodes. Ag/(0.01 M $AgNO_3$ + 0.1 M $TBAPF_6$ in CH_3CN) double junction (with pure [BMIM][NTf_2] between two frits) served as reference electrode (RE). All potentials in this paper are given vs this RE. Its potential vs aqueous SCE is 0.32 V.

Some measurements were performed with the use of another reference electrode: silver wire immersed directly into the solution. This pseudoreference electrode has been frequently employed in electrochemical studies inside ILs.[31,53] Our measurements of the Fc oxidation with this electrode (Figure 11 presents a typical example), in comparison to those with the use of our standard RE (Ag/0.01 M $AgNO_3$+AN, see above), have shown a very accurate reproduction of the whole shape of the CV curves measured versus a true reversible RE (intensity of both peaks, peak-to-peak separation, shape of increasing and

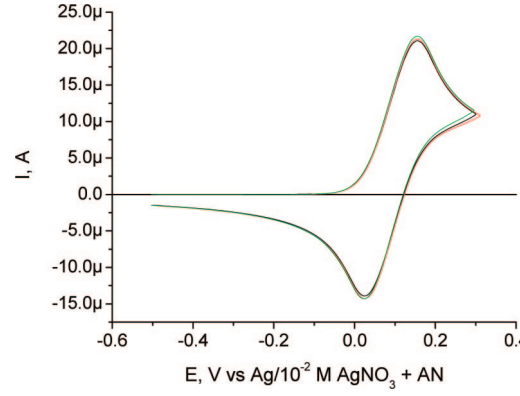

Figure 11. CVs in the IL solution of Fc (70 mM estimated concentration) measured vs true RE, Ag/0.01 M $AgNO_3$+AN (black curve), vs Ag wire (red curve), or vs Pt wire (green curve). The latter curves were registered in 20−25 min after immersion of the wire into this solution. The corresponding plots were shifted along the potential axis by 0.20 or 0.145 V in the negative direction, respectively.

decreasing branches) so that an appropriate shift along the potential axis resulted always in a perfect superposition with the CV curve versus true RE (Figure 11). However, this shift along the potential axis was gradually varying in time between 0.06 and 0.22 V (Figure 11); i.e., the interfacial potential difference between this RE and the solution was not constant.

The latter problem was of no importance for the actual study based principally on the intensity of the oxidation wave so that Ag wire was used as RE for electrochemical experiments in the Fc+IL solutions of series 3, to diminish the losses of IL in the course of the frequent electrode removal from the solution for deoxygenation.

The working electrodes (WE), Pt disk (surface area of 0.0095 cm^2) and glassy carbon (GC) disk (0.074 cm^2), were polished to a mirror finish by means of diamond suspension prior to use. Platinum wire served as counter electrode.

The electrochemical measurements were performed with a PGSTAT30 potentiostat (AUTOLAB, Ecochemie, The Netherlands). All cyclic voltammetry (CV) curves discussed below were measured with the use of the ScanGen module, i.e., under the linear potential sweep in time.

Because of very low values of the diffusion coefficients in ILs, the establishment of a stationary or a steady-state concentration profile requires a much longer period of time than that in molecular organic solvents.[29] In the conditions of cyclic voltammetry this feature may manifest itself by a stronger (than usual) diminution of the "forward" peak (anodic peak for Fc) in cycle 2 (compared to that in the first cycle) as well as by a progressive diminution of this peak in further cycles (while the CV response in organic solvents becomes stable starting already from cycle 2). Another important distinction is related to the time interval between the successive series of cycles needed to restore the initial (unperturbed) distributions of the concentrations. Since its duration depends generally on the thickness of the steady-state diffusion layer, i.e., on both the diffusion coefficients and the intensity of convective motion of the IL, it is much longer in ILs. Another affecting factor is the electrical regime imposed between the series of cycles: generally, the return to the unperturbed state is faster (for chemically reversible processes) in the potentiostatic regime (with the potential ensuring the backward transformation of the reaction product), compared to the OCP regime.

All these features are especially pronounced for processes where the reverse scan does not lead to the backward transformation of the reaction product so that the relaxation to the initial (unperturbed) state with a constant concentration profile of the reactant can only occur owing to the molecular transport of species across the diffusion layer from the bulk solution. In this context, these effects are minimized in the system under study, owing to the perfectly reversible character of the electron transfer step. Therefore, if the cathodic limit of the scans is sufficiently far from the interval of the redox transformations, the multicycle voltammetry does not reveal significant differences, similar to this process in usual media (Figure 12).

All data for cyclic voltammograms and for the anodic peak current in this paper (except for Figure 12) were registered in the course of the first cycle started after a sufficiently long relaxation of the system after the previous measurement, controlled by the amplitude of the residual cathodic current.

UV−vis spectra of Fc solutions in [BMIM][NTf_2] or various molecular organic solvents were measured in a quartz cuvette (Hellma Benelux, 2 mm optical path, volume 0.8 mL) with VARIAN Cary 50 Scan spectrophotometer within the wavelength range from 190 to 1100 nm, with subtraction of the absorbance of the pure solvent in the same cuvette.

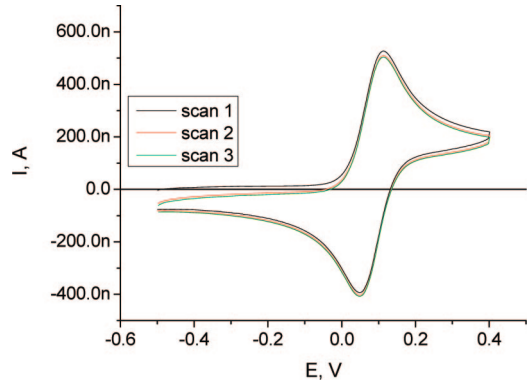

Figure 12. Multicycle CV response of Fc in IL: 1 mM Fc, Pt electrode, 100 mV/s.

For the spectral study, a portion was taken by pipet from the prepared Fc+IL solution (see Appendix 3). After the measurement the investigated portion was returned to the main working solution which was kept in the electrochemical cell under argon pressure. To avoid the loss of the IL in the course of these transfers to and from the spectral cuvette, in experimental series 1 (where the Fc+IL solution's portions were added to IL and then AN was pumped out, Appendix 3) the spectral cuvette and the pipet were rinsed several times with AN, to gather the traces of the viscous liquid from the walls and to transfer them to the main Fc+IL(+AN) solution. Then, a new portion of the Fc+AN solution was added and all AN was removed from the Fc+IL solution by vacuum treatment. This rinsing with AN was avoided in series 2 and 3 (where the Fc+IL solutions were obtained by the direct Fc dissolution in IL) and the inevitable losses of the Fc+IL solution in the course of these transfers (0.07−0.3 g per each spectral measurement) were taken into account by the measurement of the cell's weight before and after each spectral study.

The spectra of Fc solutions in IL obtained by direct dissolution of its solid powder represented a combination of the bands observed for Fc solutions in all studied solvents (AN, THF, ethanol, CH_2Cl_2, toluene, heptane) and a "tail" of a constant or a slowly decreasing intensity (above 620 nm) which was extending up to the long-wavelength limit of our measurements, 1100 nm. The latter was attributed to light scattering by solid microparticles.

We tested various treatments of these spectra to remove the "colloidal" contribution. First, we verified that all spectra of Fc+IL solutions where the colloidal tail was absent (e.g., those obtained via additions of the Fc+AN solution, Appendix 3) had identical shapes (i.e., proportional to each other). It implies that the ratio of their amplitudes is equal to the ratio of the solute Fc concentrations in the corresponding solutions. Then, such a "pure Fc spectrum" (curve 2 in Figure 13a), after multiplication by a constant (independent of wavelength) factor, was subtracted from a spectrum with the colloidal tail (curve 1 in Figure 13a), the factor being varied until the difference became independent of the wavelength in the vicinity of the principal absorption band of Fc around 440 nm (curve 3 in Figure 13a). The result of this operation was considered as justified if the difference spectrum represented a line with a smooth variation within the whole range of wavelengths, from about 350−380 to 1100 nm.

As an alternative treatment of the Fc spectra with a colloidal tail (curve 1 in Figure 13b), we extrapolated smoothly the plot from the range above 600 nm (having there a constant or a

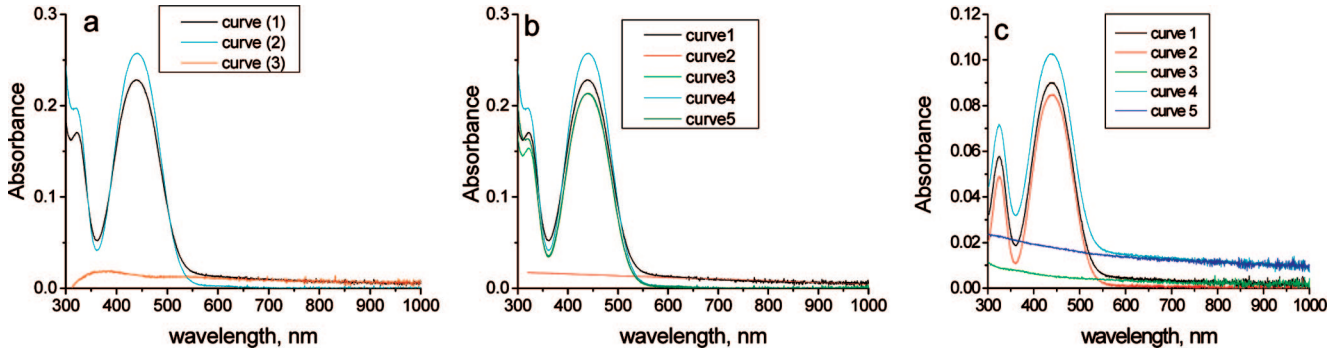

Figure 13. Illustration of three different procedures to separate a measured spectrum into the Fc contribution and a colloidal tail: (a) curve 1, measured spectrum of 8 mM (8.9 mM after taking the losses of IL into account, Appendix 3) Fc in IL with colloidal tail (series 2); curve 2, typical spectrum of Fc in IL without colloidal tail (series 1); curve 3, difference of curves 1 and curve 2 multiplied by a fitting factor (0.83); (b) curve 1, identical to curve 1 in (a); curve 2, smooth (linear) extrapolation of the colloidal tail into the range below 600 nm; curve 3, difference between curves 1 and 2; curve 4, identical to curve 2 in (a); curve 5, curve 4 multiplied by a constant factor (0.83) to reproduce the absorbance of curve 3 at 440 nm. (c) Spectra of 5 mM Fc in heptane: curve 1, initial spectrum; curve 2, spectrum measured after sedimentation of colloid; curve 3, difference between curves 1 and 2; curve 4, spectrum of well agitated solution; curve 5, difference of curves 4 and 2.

slowly decreasing intensity toward higher wavelengths) to the range below 620 nm (curve 2 in Figure 13b). Then this function was subtracted from the measured spectrum (curve 3 in Figure 13b). The difference was compared with the Fc spectrum for solutions without a tail (curve 4) multiplied by a constant factor (curve 5 in Figure 13b).

At last, as the third method (used mostly for Fc in organic solvents) for separation of the contributions from colloidal particles and the solute Fc inside the spectral curve of the initially prepared solution (curve 1 in Figure A3c), the solution was kept without stirring for several hours. The sedimentation of the colloidal component took place during this time. Then the spectrum was measured for a portion of this solution taken from its upper level (curve 2 in Figure 13c with a much weaker colloidal tail) and compared with the initial spectrum having a significant colloidal tail (curve 1). Their difference (curve 3) gave a "background absorption" considered as the difference of the colloidal absorption curves for these two portions (in accordance with this interpretation, this difference does not show any variation below 600 nm resembling the Fc bands). Vigorous ultrasonic agitation of the solution resulted in a spectrum with a much more intensive colloidal tail (curve 4 in Figure 13c). Again, the subtraction of curve 2 from this spectrum (curve 4) gives a smoothly varying curve 5 which confirms that the changes due to the agitation are merely due to increase of the intensity of the colloidal tail (curve 5 having the same shape as curve 3). It implies that the absorption of the molecularly dissolved Fc (and consequently its concentration) remains unchanged in the course of both procedures, and it can be calculated from curve 1, 2, or 4 by subtraction of the pure colloidal spectrum 3 or 5 with a properly adjusted constant factor.

Effectively, all these three treatments were successful in interpretation of all spectra of Fc solutions (where the colloidal tail was observed) as the sum of a contribution due to solute Fc and of a smoothly varying colloidal branch. Moreover, the shape of the former curve corresponded always to that for solute Fc in organic solvents while the extracted values of the absorption maximum of this contribution, A_{440}, were practically identical for all treatments, which means the same value of the concentration of solute Fc determined from these data, independent of the chosen treatment.

Appendix 3. Solution Preparation

In view of the starting hypothesis that the earlier announcements of a nonlinearity between the Fc concentration and the oxidation current might be due to a difficulty to control reliably the concentration, special attention was paid to the stage of the Fc transfer to solution.

Looking for a procedure enabling us to ensure a reliable estimation of the solute concentration on the basis of the weight and volume measurements, we tested three different ways to prepare a series of Fc solutions in IL, each of them having its merits and drawbacks, which are described in detail below.

Series 1. Series 1 of Fc+IL solutions was obtained by successive additions of certain volumes of the same Fc solution in acetonitrile (AN) into IL.

Ten millimoles per liter acetonitrile solution of Fc (Fc+AN) was first prepared. Its spectrum was typical for Fc in all studied solvents, with the proper absorbance band in the visible range having a maximum at 440 nm (section 5, Figure 7a). A slight absorption in the longer-wavelength range (above 600 nm) was also observed, with the intensity of about 0.003.

Different amounts of Fc+AN solution added into 2.5 mL of IL corresponded formally to 1, 3, 10, 20, and 40 mM Fc solutions in IL (without taking into account the presence of AN). After each addition, AN dissolved in IL was removed by vacuum pumping with magnetic stirring at room temperature for a period of 1−5 h (depending on the amount of added AN). Then the CV and spectral properties of the solution were recorded (Appendix 2).

Since the parameters of the IL (viscosity, Fc diffusion coefficient, Fc extinction coefficient, etc.) might be affected by the presence of AN, the duration needed for the removal of its principal fraction from the mixed Fc+AN+IL solution was chosen on the basis of the control of the overall weight of the cell with the solution in IL before the AN addition and after its evaporation from the IL solution.

This procedure cannot guarantee a complete removal of AN from the Fc+IL solutions. Therefore, we have analyzed potential effects of residual AN traces on the properties of the Fc solution in IL. Since the absorption band of Fc in the visible range is of practically the same shape in both solvents, with a slightly higher intensity in IL, small amounts of AN inside IL should not affect the Fc spectrum. Hypothetically, one cannot exclude a priori a much stronger change in the electrochemical signal owing to an effect of AN traces on the IL viscosity and consequently on the Fc diffusion coefficient. If it were true, one should observe a deviation from the parallelism between the two measured characteristics, current and absorbance, in the series of solutions with various Fc concentrations, contrary to our observations presented in sections 2, 4, and 6.

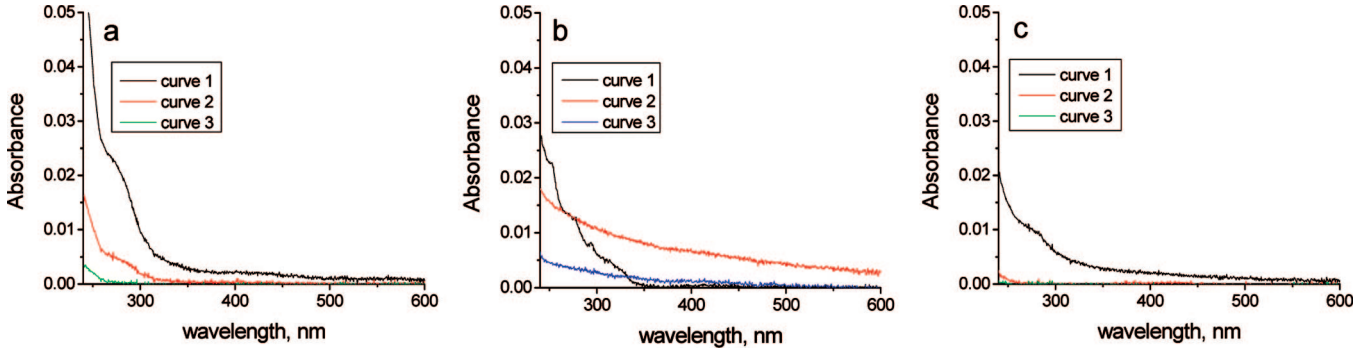

Figure 14. Spectra of pure CH_2Cl_2 after its filtration through: cotton (a), cotton + silica (b), and cotton + Celite (c). Curves 1−3 in each figure: spectra for the subsequent portions (first, second, and third, respectively) of a constant volume passed through the corresponding adsorbent.

This way of solution preparation permitted us to avoid all complications related to dissolution of the solid Fc in the IL. However, an unexpected problem arose from a sufficiently high volatility of Fc. The process of the progressive disappearance of Fc from the solution in IL was registered by repetitive measurements of its spectrum. The intensity of the Fc absorption curve diminished (without changing its shape) in the course of the vacuum or/and thermal (80° or even 50°) treatment of the cell accompanied by the solution agitation. Interestingly, identical treatment *without agitation* did not result in any change of the Fc absorption, i.e., of its concentration, probably due to an extremely slow transport of Fc molecules to the free surface of the solution. On the contrary, the process of AN evaporation from the solution went through the formation of AN bubbles inside the solution, and this was expectedly the reason of noticeable Fc losses during this stage. The diminution of the Fc concentration due to its evaporation was confirmed by a parallel diminution of the electrochemical signal as well as by the accumulation of Fc inside the trap (cooled by liquid nitrogen) together with evaporated AN, the amount of Fc in the trap being in conformity with its amount lost from its solution in IL. As additional evidence, a marked evaporation of the *solid Fc* under similar treatments has been registered by the measurement of the weight of its powder in a cell without solvent.

Since series 1 revealed a progressive diminution of the Fc amount inside the solution in the course of the combined heat + vacuum treatment, we performed a special test on a potential chemical instability of Fc in IL under these conditions, before starting series 2. A new batch of Fc was opened, and the powder was dried for 2−3 h at 45 °C for this test and the subsequent experiments.

For the stability test, a 5 mM Fc solution in IL was prepared by the direct dissolution of its powder. Then this solution was subject to various treatments: heating up to 80 °C, vacuum pumping and their combination, with or without stirring of solution. These experiments pointed out the necessity of avoiding a combination of the vacuum pumping (especially, at elevated temperature) and the solution agitation (stirring, gas bubble formation, etc.), inevitable in the procedure via a Fc+AN solution (series 1).

Series 2. Series 2 of Fc+IL solutions was prepared by direct dissolution of certain amounts of the Fc powder in IL (2.5 mL) or in the previous Fc+IL solution of this series. These amounts of immersed solid Fc were calculated to get subsequently 1, 3, 8, 16, 30, 50, and 70 mM Fc solutions (then these concentrations were corrected to take into account the losses of IL in the course of spectroscopic measurements, Appendix 2). Mechanical stirring was used for low Fc concentrations while an ultrasonic bath (with keeping the temperature below 50 °C) was applied for higher concentrations. After the disappearance of visible solid particles, the electrochemical and spectroscopic studies were performed with each solution. The solutions were kept in the electrochemical cell under argon pressure.

A "colloidal branch" of the spectrum in the range above 600 nm with a constant or a slowly decreasing intensity was more pronounced for solutions of series 2 than for corresponding concentrations in series 1. The repeated spectral measurements either after the solution storage inside the cuvette without stirring or after the solution centrifugation resulted in a diminution of this absorption above 600 nm while the ultrasonic treatment or stirring enhanced it; i.e., these changes originated merely from sedimentation and resolubilization of solid microparticles.

We cannot specify whether these particles (observed mostly in series 2, i.e., with the use of the new batch of solid Fc) represent a foreign insoluble material or very slowly dissolving Fc grains. The former seems to be more probable since the colloidal branch was also observed in Fc solutions in all tested solvents: AN, THF, heptane, C_2H_5OH, C_2H_5OH + 1 M $LiClO_4$ (imitating charged species of IL), CH_2Cl_2, and toluene, even after ultrasonic treatment.

Series 3. In an attempt to avoid the appearance of these solid microparticles in the solution, the Fc solution in freshly distilled CH_2Cl_2 was filtrated through an adsorbent.

To trace possible contaminations extracted from the adsorbent, the passage of pure solvent through various adsorbents (Celite, cotton, carbon, and silica; their combinations: cotton + silica, cotton + carbon, cotton + silica + carbon, etc.) was studied first, with spectrophotometric control of the filtrate (Figure 14). In all cases new absorption bands were observed in the near-UV and/or adjacent visible ranges, compared to the spectrum of pure solvent. The best result (minimum contamination bands) was obtained for the second portion of the solvent passed through Celite: the spectrum of the first portion showed an increase of absorption in the range below 300 nm, the absorption of the next subsequent portions was rather weak (Figure 14c).

On the basis of these findings, the saturated Fc solution in CH_2Cl_2 (curve 1 in Figure 15) was filtrated through Celite + cotton layer. Each time a portion of pure solvent (equal to that in Figure 14c) was passed through a fresh portion of Celite, then the Fc + CH_2Cl_2 solution was filtrated through the same adsorbent layer. This operation was repeated three times with each portion of the Fc + CH_2Cl_2 solution. The solution at the end of the whole procedure exhibited a typical Fc spectrum, without any colloidal branch (Figure 15, curve 2). The difference of the spectral curves (curve 3 in Figure 15) corresponds to a purely colloidal tail.

Then the filtered solution was evaporated under vacuum at room temperature during several hours, the process being

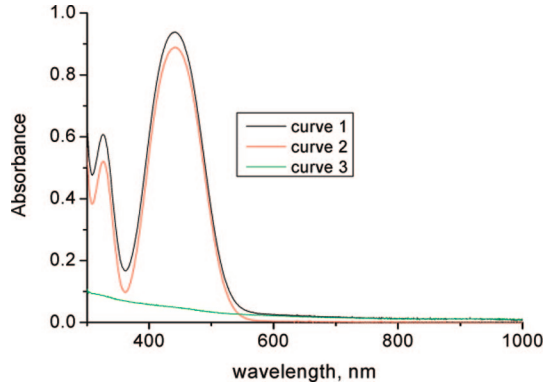

Figure 15. Spectra of saturated Fc solution in CH_2Cl_2: curve 1, solution after the dissolution of Fc; curve 2, the same solution after its filtration through Celite (after correction for the solvent evaporation; curve 3, difference of curves 1 and 2).

controlled by the weight measurement, until its stabilization. This portion of Fc was used for its direct dissolution in IL, with the use of ultrasonic bath, to prepare series 3 of Fc+IL solutions with expected concentrations of 1, 3, 10, and 20 mM.

It has been reported earlier[54] that an intensive and prolonged ultrasonic treatment of imidazolium ILs (20 kHz, 60 W/cm^2, 3 h duration, with temperature increase up to 85 or 135 °C) led to darkening of the liquid, with the change from colorless to amber color, indicating some decomposition of IL. Therefore, the conditions in our treatment, 48 kHz, output power 50 W, 30−80 min (Bransonic 220, Germany), were chosen to limit the temperature to 50 °C.

The electrochemical and spectroscopic measurements as well as the control of the IL losses in series 3 of solutions were carried out in the same manner as described in series 2. The only methodical change was the use of Ag wire as RE in order to diminish the amount of IL lost because of the necessity to extract our standard double-junction RE (Appendix 2) from the solution after each electrochemical measurement.

Even though the spectrum of the filtrated Fc+CH_2Cl_2 solution did not show visible contaminations or Fc oxidation, we had to suppose that some substance(s) (not visible in the spectrum of this solution) had been extracted in the course of this filtration. This conclusion is based on the observation that after the Fc dissolution in IL an additional absorption band (maximum at 620 nm) was observed which increased in parallel with the Fc concentration. As a result, the color of the solution became yellow-greenish starting from 3 mM. The vacuum pumping resulted again in Fc losses, without removal of the contamination(s). Its presence in the solution did not affect the electrochemical signal or the principal absorption band of Fc in the range of 400−500 nm (some changes were observed near the absorption minimum at 360 nm, see Figure 8a in section 6). The spectra for this series were successfully decomposed into the bands of Fc and the contamination, with the use of the spectrum of the Fc+IL solution determined in series 1.

One should emphasize that all background corrections (subtractions of the colloidal branch) of the measured spectra for Fc+IL solutions did not change significantly the absorption properties in the range of the Fc band, the maximum correction being well below 10% so that this procedure was merely designed to increase the precision of the results. As for electrochemical data, the subtraction of the EDL capacitance contribution led to a marked effect only for the minimal Fc concentration. For highest Fc concentrations (starting from about 10 mM) the Ohmic losses became significant, owing to the solution resistance (about 2 kΩ for Pt electrode), so that the mode of the IR compensation of the potentiostat was applied.

Because of the necessity to carry out numerous steps, especially for extended vacuum pumping, each series required several days of experiments, despite all means used for their acceleration. No apparent changes in electrochemical or spectroscopic properties were noticed on this time scale. However, a more extended storage of such solutions of series 2, for a month or longer (even in Schlenk tube under Ar pressure, protected from light), revealed a change of its color (from yellow to greenish one) and correspondingly of its spectrum in which a new band near 620 nm was progressively increasing (as a shoulder in 1 month, becoming a peak after 2 months), analogous to that observed for solutions of series 3 (section 6, Figure 8a, but with a much faster evolution at the scale of several hours), probably due to partial oxidation of Fc to Fc^+.[46,47]

References and Notes

(1) Wilkes, J. S. *J. Mol. Catal. A: Chem.* **2004**, *214*, 11.
(2) Beste, Y.; Eggersmann, M.; Schoenmakers, H. *Chem. Ing. Tech.* **2005**, *77*, 1800.
(3) Dupont, J.; Suarez, P. A. Z. *Phys. Chem. Chem. Phys.* **2006**, *8*, 2441.
(4) Fredlake, C. P.; Crosthwaite, J. M.; Hert, D. G.; Aki, S. N. V. K.; Brennecke, J. F. *J. Chem. Eng. Data* **2004**, *49*, 954.
(5) Earle, M. J.; Esperança, J. M. S. S.; Gilea, M. A.; Canongia Lopes, J. N.; Rebelo, L. P. N.; Magee, J. W.; Seddon, K. R.; Widegren, J. A. *Nature* **2006**, *439*, 830.
(6) Meindersma, G. W.; Podt, A. J. G.; de Haan, A. B. *Fuel Process. Technol.* **2005**, *87*, 59.
(7) Jacquemin, J.; Costa Gomes, M. F.; Husson, P.; Majer, V. *J. Chem. Thermodyn.* **2006**, *38*, 490.
(8) Chowdhury, S.; Mohan, R. S.; Scott, J. L. *Tetrahedron* **2007**, *63*, 2363.
(9) Welton, T. *Chem. Rev.* **1999**, *99*, 2071.
(10) Chiappe, C.; Pieraccini, D. *J. Phys. Org. Chem.* **2005**, *18*, 275.
(11) Dupont, J.; de Souza, R. F.; Suarez, P. A. Z. *Chem. Rev.* **2002**, *102*, 3667.
(12) Wasserscheid, P.; Keim, W. *Angew. Chem., Int. Ed.* **2000**, *39*, 3772.
(13) Jain, N.; Kumar, A.; Chauhan, S.; Chauhan, S. M. S. *Tetrahedron* **2005**, *61*, 1015.
(14) Binnemans, K. *Chem. Rev.* **2007**, *107*, 2592.
(15) Pârvulescu, V. I.; Hardacre, C. *Chem. Rev* **2007**, *107*, 2615.
(16) Van Randwijk, F.; Sheldon, R. A. *Chem. Rev.* **2007**, *107*, 2757.
(17) Galinski, M.; Lewandowski, A.; Stepniak, I. *Electrochim. Acta* **2006**, *51*, 5567.
(18) Buzzeo, M. C.; Evans, R. G.; Compton, R. G. *ChemPhysChem* **2004**, *5*, 1106.
(19) Fernicola, A.; Scrosati, B.; Ohno, H. *Ionics* **2006**, *12*, 95.
(20) Brooks, C. A.; Doherty, A. P. *J. Phys. Chem. B* **2005**, *109*, 6276.
(21) Brooks, C. A.; Doherty, A. P. *Electrochem. Soc. Proc.* **2002**, *19*, 900.
(22) Lagrost, C.; Carrié, D.; Vaultier, M.; Hapiot, P. *J. Phys. Chem. A* **2003**, *107*, 745.
(23) Endres, F. *ChemPhysChem* **2002**, *3*, 144.
(24) Innis, P. C.; Mazurkiewicz, J.; Nguyen, T.; Wallace, G. G.; MacFarlane, D. *Curr. Appl. Phys.* **2004**, *4*, 389.
(25) Pringle, J. M.; Efthimiadis, J.; Howlett, P. C.; Efthimiadis, J.; MacFarlane, D. R.; Chaplin, A. B.; Hall, S. B.; Officer, D. L.; Wallace, G. G.; Forsyth, M. *Polymer* **2004**, *45*, 1447.
(26) Zein El Abedin, S.; Borissenko, N.; Endres, F. *Electrochem. Commun.* **2004**, *6*, 422.
(27) Schneider, O.; Bund, A.; Ispas, A.; Borissenko, N.; Zein El Abedin, S.; Endres, F. *J. Phys. Chem. B* **2005**, *109*, 7159.
(28) Zhang, J.; Bond, A. M. *Analyst (Cambridge)* **2005**, *130*, 1132.
(29) Boxall, D. L.; O'Dea, J. J.; Osteryoung, R. A. *J. Electrochem. Soc.* **2002**, *149*, E468.
(30) Nagy, L.; Gyetvai, G.; Kollar, L.; Nagy, G. *J. Biochem. Biophys. Methods* **2006**, *69*, 121.
(31) Rogers, E. I.; Silvester, D. S.; Poole, D. L.; Aldous, L.; Hardacre, C.; Compton, R. G. *J. Phys. Chem. C* **2008**, *112*, 2729.
(32) Compton, D. L.; Laszlo, J. A. *J. Electroanal. Chem.* **2002**, *520*, 71.
(33) Schröder, U.; Wadhawan, J. D.; Compton, R. G.; Marken, F.; Suarez, P. A. Z.; Consorti, C. S.; de Souza, R. F.; Dupont, J. *New J. Chem.* **2000**, *24*, 1009.
(34) Koepp, H. M.; Wendt, H.; Strehlow, H. Z. *Electrochemistry* **1960**, *64*, 483.

(35) Hultgren, V. M.; Mariotti, A. W. A.; Bond, A. M.; Wedd, A. G. *Anal. Chem.* **2002**, *74*, 3151.
(36) Brooks, C. A.; Doherty, A. P. *Electrochem. Commun.* **2004**, *6*, 867.
(37) Eisele, S.; Schwarz, M.; Speiser, B.; Tittel, C. *Electrochim. Acta* **2006**, *51*, 5304.
(38) Fietkau, N.; Clegg, A. D.; Evans, R. G.; Villagran, C.; Hardacre, C.; Compton, R. G. *ChemPhysChem* **2006**, *7*, 1041.
(39) Fuller, J.; Carlin, R. T.; Osteryoung, R. A. *J. Electrochem. Soc.* **1997**, *144*, 3881.
(40) Boxall, D. L.; Osteryoung, R. A. *J. Electrochem. Soc.* **2004**, *151*, E41.
(41) Boxall, D. L.; Osteryoung, R. A. *J. Electrochem. Soc.* **2002**, *149*, E185.
(42) Sweeny, B. K.; Peters, D. G. *Electrochem. Commun.* **2001**, *3*, 712.
(43) Nicholson, R. S. *Anal. Chem.* **1966**, *38*, 1406.
(44) Wilkinson, G.; Rosenblum, M.; Whiting, M. C.; Woodward, R. B. *J. Am. Chem. Soc.* **1952**, *74*, 2125.
(45) Emel'yanenko, V. N.; Verevkin, S. P.; Krol, O. V.; Varushchenko, R. M.; Chelovskaya, N. V. *J. Chem. Thermodyn.* **2007**, *39*, 594.
(46) Sohn, Y. S.; Hendrickson, D. N.; Gray, H. B. *J. Am. Chem. Soc.* **1970**, *92*, 3233.
(47) Bohari, M. Y.; Shabbir, A. T. *Sci. Int. (Lahore, Pak.)* **1994**, *6*, 125.
(48) Ju, H.; Ye, B.; Gu, J. *Sensors* **2004**, *4*, 71.
(49) Rosenblum, M.; Santer, J. O.; Howells, W. G. *J. Am. Chem. Soc.* **1963**, *85*, 1450.
(50) Akihiro, N.; Kikuko, H.; Watanabe, M. *J. Phys. Chem. B* **2001**, *105*, 4603.
(51) Tokuda, H.; Hayamizu, K.; Ishii, K.; Susan, M. Abu. Bin. Hasan.; Watanabe, M. *J. Phys. Chem. B* **2004**, *108*, 16593.
(52) Bonhôte, P.; Dias, A.-P.; Papageorgiou, N.; Kalyanasundaram, K.; Grätzel, M. *Inorg. Chem.* **1996**, *35*, 1168.
(53) Anthony, G. W. *Anal. Chem.* **2002**, *74*, 3151.
(54) Oxley, J. D.; Prozorov, T.; Suslick, K. S. *J. Am. Chem. Soc.* **2003**, *12195*, 11138.

JP809095Q